Green Chemistry

Accepted Manuscript

This article can be cited before page numbers have been issued, to do this please use: D. K. Mishra, H. J. Lee, J. Kim, H. Lee, J. K. Cho, Y. Suh and Y. J. Kim, *Green Chem.*, 2017, DOI: 10.1039/C7GC00027H.

ROYAL SOCIETY OF CHEMISTRY

rsc.li/green-chem

View Article Online
DOI: 10.1039/C7GC00027H

Green Chemistry

COMMUNICATION

$MnCo_2O_4$ Spinels Supported Ruthenium Catalyst for Air-Oxidation of HMF to FDCA under Aqueous Phase and Base-Free Conditions†

Received 00th January 20xx,
Accepted 00th January 20xx

DOI: 10.1039/x0xx00000x

www.rsc.org/

Dinesh Kumar Mishra,[a] Hye Jin Lee,[b] Jinsung Kim,[c] Hong-Shik Lee,[a] Jin Ku Cho,[a,b] Young-Woong Suh[c] and Yong Jin Kim[a,b,*]

A new class of $MnCo_2O_4$ spinels supported Ru catalyst, Ru/$MnCo_2O_4$, was exploited to afford highest yield of FDCA (99.1%) from base-free air-oxidation of HMF in water. Catalyst Ru/$MnCo_2O_4$ having both Lewis and Brønsted acidic active sites greatly enhanced the FDCA yield. The catalyst was recyclable up to five successive runs without considerable loss of its original activity.

Over recent decades, there has been a growing interest in biomass conversion to the molecules known as building block platform chemicals[1] because they have multiple functionalities in their structures which are suitable for further chemical transformation into value-added chemicals.[2-5] For example, 5-hydroxymethylfurfural (HMF) is one of the key platform molecules derived from sugars or cellulose,[6-10] and is now known as a reputable substrate for the production of a variety of chemicals such as maleic anhydride (MA), 2,5-diformylfuran (DFF), and 2,5-furandicarboxylic acid (FDCA).[11-15] Among them, FDCA has received significant attention as it can be used as polymer building block for the synthesis of bio-based polymers such as polyamides, polyesters, and polyurethanes.[16-18] Moreover, the FDCA has high potential as a replacement of terephthalic acid (TPA), the monomer of polyethylene terephthalate (PET).[19, 20] One example of the promising bio-based polymers using FDCA is polyethylene 2,5-funrandicarboxylate (PEF) due to the good barrier properties.[14, 21, 22] Therefore, the substitution of TPA with FDCA constitutes substantial step forward in terms of sustainability as well as opening a new bio-based chemical market.

Earlier, HMF could be oxidized to FDCA via the formation DFF as an intermediate with stoichiometric oxidants $KMnO_4$, or HNO_3,[23] and enzyme.[24-26] Later, a number of publications describe the HMF oxidation to produce FDCA wherein noble metals such as Au, Pt, Pd, and Ru based catalysts are used.[27-35] To afford high yield of FDCA, Au based catalysts like Au/TiO_2[27], Au/CeO_2[28] and Au/hydrotalcites (HT)[36] are used. Other metals like Pt-based catalysts [29, 33, 35] were found to show better performances than Au for aerobic oxidation of HMF to FDCA. However, supported Au- and Pt-based catalysts often require excess amounts of inorganic base such as NaOH or Na_2CO_3. An interesting example of the catalysts for base-free conversion of HMF to FDCA includes hydrotalcites supported Au catalyst[30] which gave high yield of FDCA, 99% and 81% with molecular oxygen and air, respectively. However, the FDCA yield decreased sharply to 92% in the second run, and 90% after third run. Another type of bimetallic catalyst, carbon nanotube supported Au-Pd alloy system reported by wan et al., gave a 94% of FDCA yield at 100 °C after 12 h, however, this process needed pure O_2 as oxidant to get high yield.[31] Some other examples of Pt-based catalysts such as Pt/C[29] and Pt/ZrO_2[33] were also evaluated in HMF oxidation but these processes still suffer from the high cost of metal.

Economical point of view, the use of less expensive ruthenium metal is quite advantageous. As for HMF oxidation, Ru-based catalysts have been mainly concerned with the oxidation of HMF for producing DFF in organic solvents [14, 37, 38] and for FDCA in aqueous phase. $Ru(OH)_x$ on a variety of metal oxides[39, 40] and another type of catalyst system, $Ru(OH)_x$ dispersed in ionic liquids[41] have been reported for this purpose. Recently, Yi et al. reported a catalytic transformation of HMF into FDCA with 88% yield over commercial Ru/C catalyst in base-free aqueous phase.[32] More recently, a new catalytic system consisting of covalent triazine frameworks (CTFs) and ruthenium (Ru/CTFs) was successfully applied to HMF oxidation to produce FDCA with 77.6% yield at 140 °C and 20 bar of air.[34] Although both Ru/C and Ru/CTFs showed promising recyclability of the catalyst, the low yield of FDCA still remains as regrettable.

---

[a] *Green Process Material Research Group, Korea Institute of Industrial Technology (KITECH), 89, Yangdaegiro-gil, Ipjang myeon, Cheonan-si 331-822, Republic of Korea. *E-mail: yjkim@kitech.re.kr*

[b] *Korea University of Science and Technology (UST), 176 Gajeong-dong, 305-350, Yuseong-gu, Daejeon, Republic of Korea.*

[c] *Department of Chemical Engineering, Hanyang University, Seoul 133-791, Republic of Korea.*

†Electronic Supplementary Information (ESI) available: [Catalyst preparation, Characterization-figures (NH_3TPD, TEM, TEM-EDS, XPS, and XRD), Tables (EDS, BET, CO chemisorption, and ICP-ES,), & FDCA purification- ^{1}H-NMR, and ^{13}C-NMR of purified FDCA]. See DOI: 10.1039/x0xx00000x

View Article Online
DOI: 10.1039/C7GC00027H

A hitherto unreported heterogeneous catalyst, $MnCo_2O_4$ spinels supported ruthenium, $Ru/MnCo_2O_4$, is investigated to produce FDCA from base-free air-oxidation of HMF in water used as greenest solvent. Earlier, $MnCo_2O_4$ spinels have been used as electrode materials for the specific purpose only in oxygen reduction reaction (ORR) and oxygen evolution reaction (OER).[42] Prompted by the specific properties of $MnCo_2O_4$, and the activities of Co and Mn based homogeneous catalyst systems such as $Co(OAc)_2/Mn(OAc)_2/HBr$ used in HMF oxidation[43] and $CoBr_2/MnBr_2$ in *para*-xylene oxidation,[44] $MnCo_2O_4$ supported ruthenium nanoparticles is synthesized and applied as heterogeneous nano catalyst for HMF oxidation. To the best of our knowledge, there is no report so far on the use of $MnCo_2O_4$ spinels supported ruthenium as nano catalyst in HMF oxidation. $MnCo_2O_4$ is composed of a mixed oxide with Mn and Co having multiple valance states that acquires spinel structure where the both metal cations are distributed in tetrahedral and octahedral sites.[42] The ratio of all metal contents in $MnCo_2O_4$ and its corresponding ruthenium catalyst are determined by EDS and ICP (Table S1).

The formation of FDCA requires the oxidation of both hydroxyl and aldehyde groups in HMF to form carboxylic groups. Supported noble metal-based catalysts are generally active for the oxidation of organic molecules that include aldehydes and alcohols. Thus, we investigated the catalytic behaviors of least expensive noble metal ruthenium-based catalysts in HMF oxidation to produce FDCA under base-free aqueous condition, and results are summarized in table 1. Catalyst $Ru(4\%)/MnCo_2O_4$, exhibits the highest yield of FDCA (99.1%) at almost complete HMF conversion (entry 1). As for by-products, only small amount of 5-formylfuran-2-carboxylic acid (FFCA) was found in the product mixture. The productivity, defined as production of FDCA (mmol) per unit gram of ruthenium per unit hour, is highest (33 $mmol \cdot g^{-1} \cdot h^{-1}$). These outstanding results towards the highest yield/productivity of FDCA are attributed to the availability of both Lewis and Brønsted acid sites on the surface of the catalyst $Ru(4\%)/MnCo_2O_4$, which is confirmed by NH_3-TPD (Figure S1, & Table S2). The NH_3-TPD profile of $Ru(4\%)/MnCo_2O_4$ clearly shows two peaks, a peak at lower temperature 224 °C is ascribed to the desorption of NH_4^+ bound to the Brønsted acid sites (10.7 $mmol \cdot g^{-1}$), and another new peak at higher temperature 511 °C is originated from the desorption of Lewis acid-coordinated NH_3 (7.3 $mmol \cdot g^{-1}$), i.e., total 18 $mmol \cdot g^{-1}$ (Table S2). On contrary, the support material, $MnCo_2O_4$ has only Brønsted acidity (8.2 $mmol.g^{-1}$). The NH_3-TPD profile of $MnCo_2O_4$ shows a couple of peaks in the temperature range from 100 °C to 350 °C which are arisen from desorption of NH_4^+ bound to the Brønsted acid sites. While, another support $CoMn_2O_4$ (Mn:Co = 2:1), as compared to $MnCo_2O_4$ (Mn:Co= 1:2), has higher Brønsted acid sites (11.2 $mmol.g^{-1}$) (Table S2). However, the $Ru(4\%)/CoMn_2O_4$ resulted in only 82.2% yield of FDCA with the large remaining of FFCA (17.6%) (entry 2). It is noteworthy to mention that $MnCo_2O_4$, in comparison to $CoMn_2O_4$, is superior based on the fact that the crystalline structure of $MnCo_2O_4$ is cubic system while, $CoMn_2O_4$ is body-centered tetragonal phase, and has distorted spinels structures.[42]

Table 1. Catalyst screening in HMF oxidation.

Entry	Catalyst	HMF/Ru (Ratio)	C_{HMF} (%)	Y_{FDCA} (%)	Y_{FFCA} (%)	Y_{DFF} (%)	FDCA Productivity $(mmol. h^{-1} g_{Ru}^{-1})$
1[a]	$Ru(4\%)/MnCo_2O_4$	33.6	100	99.1	0.9	0.0	33.0
2[a]	$Ru(4\%)/CoMn_2O_4$	33.6	100	82.2	17.6	0.0	27.4
3[a]	$Ru(4\%)/MnCo_2CO_3$	33.6	99.9	69.9	30.0	0.0	23.3
4[a]	$Ru(4\%)/MnO_2$	33.6	98.8	31.1	46.5	22.0	10.4
5[a]	$Ru(4\%)/CoO$	33.6	91.1	17.8	55.2	16.4	5.9
6[b]	$MnCo_2O_4$	-	57.8	10.9	21.4	23.9	0.0
7[a]	$Ru(4\%)/MgAl_2O_4$	10	100	36.5	56.5	6.5	3.7
8[c]	$Ru(5\%)/C$	10	100	45.3	54.7	0.0	4.5
9[c]	$Ru(4\%)/MnCo_2O_4$	10	100	60.8	39.2	0.0	6.1

Reaction conditions: [a]HMF= 2 mmol, solvent (H_2O)= 20 mL, t= 10 h, T= 120 °C, $P_{(air)}$= 2.4 MPa., [b]Catalyst= 0.2 g. [c]$P_{(air)}$= 0.7 MPa.

Moreover, $MnCo_2O_4$ also has Brønsted acidity with larger surface area (151 m^2/g) than that of $CoMn_2O_4$ (89.5 m^2/g) (Table S2 and S3). It is also believed that $MnCo_2O_4$ has a strong adsorption affinity of oxygen associated with well interacted manganese & cobalt oxides species.[45,46] Meanwhile, loading 4% of ruthenium with particle size (3.4 nm) on the $MnCo_2O_4$ leads to subsequent decrease in the surface area from 151.1 m^2/g to 135.4 m^2/g (Table S3).

A carbonate species ($MnCo_2CO_3$) is the precursor of $MnCo_2O_4$. The lower activity (FDCA with 69.9% yield, entry 3) of $Ru/MnCo_2CO_3$ than $Ru/MnCo_2O_4$ is likely responsible for the non-cubic spinels structures arising from the lack of oxygen molecule.[42] To ensure the importance of spinel structure, two sets of simple metal oxides (MnO_2 and CoO) were tested as support with ruthenium in the same HMF oxidation (entries 4 and 5). The results, much lower yields of FDCA (31.1 and 17.8%) obtained from Ru/MnO_2 and Ru/CoO, respectively, clearly indicate the role of spinel structure in the support with the ruthenium catalyst. It is interesting to note that the spinel $MnCo_2O_4$ itself with Brønsted acidity (8.2 $mmol.g^{-1}$) could give 10.9% of FDCA yield at 57.8% of HMF conversion. When comparing the catalytic activity of $Ru/MnCo_2O_4$ with the ruthenium catalysts supported by two different type, i.e., a typical $MgAl_2O_4$ spinels and commercial charcoal, they delivered only 28.3% and 45.3% of FDCA yield, respectively at the identical reaction conditions (entries 7 and 8). Nevertheless, it is important to mention that our catalyst ($Ru/MnCo_2O_4$) was able to produce the FDCA with higher yield (60.8%) than Ru/C even at low air pressure (0.7 MPa) (entry 9), which corresponds to 7.3 times higher productivity.

The morphology of $MnCo_2O_4$ microspheres and its precursor were investigated by SEM (Figure 1) and TEM (Figure S2). As shown in Figure 1a, the diameter of $MnCo_2O_4$ microspheres is in the range of 2.0-4.0 μm. Figure 1b indicates that a microsphere is formed by the aggregation of interconnected nanoparticles with typical sizes ranging from around 45-50 nm. Figure 1c and 1d show the SEM images and its corresponding high magnification of its precursor ($MnCo_2CO_3$), respectively. From these images, it is clear to state that the morphology of $MnCo_2O_4$ is different from that of precursor as a result of transformation of carbonate species into $MnCo_2O_4$ spinels. TEM with EDS mapping images of all elements including ruthenium are also displayed in figure S3.

View Article Online
DOI: 10.1039/C7GC00027H

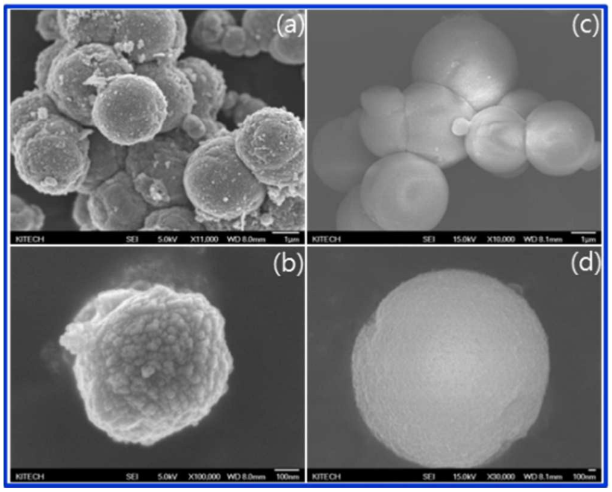

Figure 1. SEM image of $MnCo_2O_4$-(a), high magnified SEM image of $MnCo_2O_4$-(b), SEM image of $MnCo_2CO_3$-(c), and high-magnified SEM image of $MnCo_2CO_3$-(d).

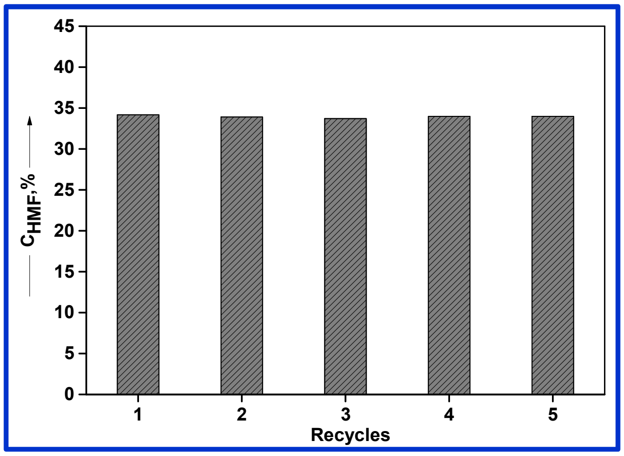

Figure 2. Catalyst recycling studies on $Ru/MnCo_2O_4$ in the HMF oxidation under kinetic-controlled regime.

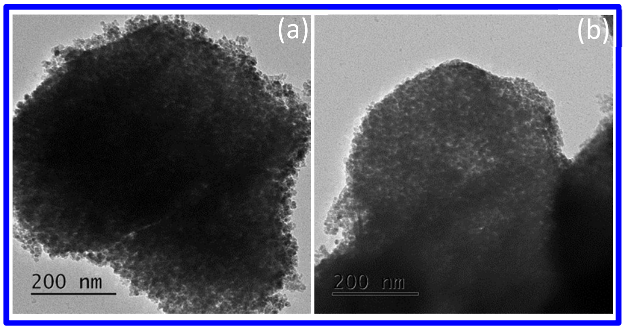

Figure 3. TEM images of fresh catalyst Ru(4%)/$MnCo_2O_4$-(a), and reused catalyst Ru(4%)/$MnCo_2O_4$ after five cycles-(b).

The information on the valence states of Mn and Co in $MnCo_2O_4$ spinels is further investigated by X-ray photoelectron spectroscopy (XPS) and the spectra are given in figure S4. The survey spectrum exhibits the presence of Co, Mn, O, and Ru (figure S4a). The characteristic peaks $2p_{3/2}$ and $2p_{1/2}$ appeared at ~780 eV and ~796 (eV) are responsible for the coexistence of Co(II) and Co(III) (figure S4b). It is reported earlier that Co(II) and Co(III) having same binding energies, can be distinguished by their Co $2p_{1/2}$–$2p_{3/2}$ spin–orbit level energy spacing (i.e. BE=15 eV)[42, 47]. Mn 2p spectrum (figure S4c) shows the two peaks $2p_{3/2}$ and $2p_{1/2}$ appeared at ~642.0 and ~654 eV, which correspond to the Mn(II) and Mn(III), respectively. The O 1s spectrum (figure S4d) indicates that O atoms are present in the spinel structure lattice.

For the confirmation of metallic ruthenium, the spectra of Ru 3d and Ru 3p are presented in figure S4(e) and S4(f), respectively. In figure S4(e), the two peaks $3d_{3/2}$ and C 1S in the spectrum of Ru 3p region (from 278 to 300 eV) overlapped at around 283 eV which makes it difficult to analyse this region, while a $3p_{3/2}$ peak at ~463 (eV) in the spectrum of Ru 3p region (from 455 to 480 eV) clearly indicates the existence of metallic ruthenium. The structural arrangements of Mn and Co in cubic spinels structure is also confirmed by XRD (Figure S5).

To test the reusability of the catalyst, the $Ru/MnCo_2O_4$ was recycled in five successive runs in the kinetic-controlled regime, i.e. under the conditions of low conversion. After each reaction, the catalyst was thoroughly washed with methanol, dried in oven at 45 °C under vacuum for 10 h and then reused. As shown in Figure 2, even after five cycles, the results pointed out that there was no significance change in rate of HMF transformation (34.2% conversion of HMF within short time as 15 min). It is noteworthy to mention that FDCA yield was low as 4.5% at 34.2% conversion of HMF (cycle #1), and there were remained two intermediates, DFF with 14.1% and FFCA with 15.5% yields. The structural stability of reused catalyst Ru(4%)/$MnCo_2O_4$ after five cycles is investigated by TEM. On comparing the TEM images of fresh catalyst Ru(4%)/$MnCo_2O_4$ (Figure 3a) and reused catalyst Ru(4%)/$MnCo_2O_4$ after five cycles (Figure 3b), the morphology looks like indicating no discernible change in structural stability of reused catalyst Ru(4%)/$MnCo_2O_4$ even after five cycles. Also, ICP analysis reveals that there was no ruthenium metal leaching in the product solution (Table S4).

In summary, a highly active and recyclable heterogeneous catalyst, $Ru/MnCo_2O_4$, was developed and applied to produce highest yield of FDCA (99.1%) form HMF oxidation in aqueous phase under base-free conditions with air used as oxidant. Both Lewis and Brønsted acidic active sites on the surface of Ru(4%)/$MnCo_2O_4$ were playing important role to enhance the yield/productivity of FDCA. During reaction, it was also observed that HMF oxidation proceeded via DFF and FFCA formation rather than HMFCA formation to form FDCA. Moreover, the use of catalyst heterogeneous catalyst $Ru/MnCo_2O_4$ for the conversion of biomass derived HMF to FDCA with high yield under base free conditions, is in favour of environmentally benign protocol.

The oxidation of HMF to produce FDCA was carried out in a 100 mL of high-pressurized stainless steel reactor equipped with a magnetic stirrer and an electrical heater. In all experiments, the reactor was charged with HMF (2 mmol), an appropriate water (15 mL), and the required amount of catalyst. After that, 0.5 MPa of synthetic air was purged into the reactor to evacuate atmospheric air from reaction mixture three times. The reactor was then pressurized up to desired pressure of air, and heated up to desired temperature with stirring rate 650 rpm. Throughout the entire reaction time, the final pressure of air into the reactor (2.4 MPa) was maintained by using a gas reservoir equipped with a back-pressure regulator and a pressure transducer. At the end of reaction, the product mixture was allowed to cool down at room

View Article Online
DOI: 10.1039/C7GC00027H

temperature and certain amount of CH_3OH was added. The solid catalyst and product solution were separated out by filtration method. The liquid samples were analyzed by using High Performance Liquid Chromatography (HPLC) instrument (Agilent Technologies 1200 series, Bio-Rad Aminex HPX-87 H pre-packed column, and UV-detector). H_2SO_4 (0.0005 M) in water was used as mobile phase. The yield and selectivity were calculated based on conversion of HMF and confirmed by calibration of standard solution of the products and reactant. The structure of pure FDCA was confirmed by ^{1}H-NMR (in DMSO-d_6 solvent) and ^{13}C-NMR (in DMSO-d_6 solvent) (Figure S7 and S8).

Acknowledgements

This work was supported by the Ministry of Science, ICT & Future Planning as “Fusion Research Program for Green Technologies (2012M3C1A1054497)” through the National Research Foundation of Korea and by the Korea Institute of Industrial Technology as “Technology for [C1+C5]-based Core Material”.

Notes and references

1. J. J. Bozell and G. R. Petersen, *Green Chemistry*, 2010, **12**, 539-554.
2. J. N. Chheda, G. W. Huber and J. A. Dumesic, *Angewandte Chemie International Edition*, 2007, **46**, 7164-7183.
3. A. Corma, S. Iborra and A. Velty, *Chemical Reviews*, 2007, **107**, 2411-2502.
4. P. Gallezot, *Chemical Society Reviews*, 2012, **41**, 1538-1558.
5. R.-J. van Putten, J. C. van der Waal, E. de Jong, C. B. Rasrendra, H. J. Heeres and J. G. de Vries, *Chemical Reviews*, 2013, **113**, 1499-1597.
6. X. Cao, S. P. Teong, D. Wu, G. Yi, H. Su and Y. Zhang, *Green Chemistry*, 2015, **17**, 2348-2352.
7. S. Dutta, S. De and B. Saha, *ChemPlusChem*, 2012, **77**, 259-272.
8. L. Lai and Y. Zhang, *ChemSusChem*, 2011, **4**, 1745-1748.
9. W.-H. Peng, Y.-Y. Lee, C. Wu and K. C. W. Wu, *Journal of Materials Chemistry*, 2012, **22**, 23181-23185.
10. S. P. Teong, G. Yi, H. Zeng and Y. Zhang, *Green Chemistry*, 2015, **17**, 3751-3755.
11. J. E. Holladay, J. F. White, J. J. Bozell and D. Johnson, *Top Value-Added Chemicals from Biomass - Volume II—Results of Screening for Potential Candidates from Biorefinery Lignin*, Report PNNL-16983; Other: BM0102070; TRN: US200805%%262 United States 10.2172/921839 Other: BM0102070; TRN: US200805%%262 PNNL English, ; Pacific Northwest National Laboratory (PNNL), Richland, WA (US), 2007.
12. J. Lan, J. Lin, Z. Chen and G. Yin, *ACS Catalysis*, 2015, **5**, 2035-2041.
13. T. Werpy and G. Petersen, *Top Value Added Chemicals from Biomass: Volume I -- Results of Screening for Potential Candidates from Sugars and Synthesis Gas*, Report DOE/GO-102004-1992; TRN: US200427%%671 United States10.2172/15008859TRN: US200427%%671Tue Feb 12 21:52:38 EST 2008NRELEnglish, 2004.
14. Z. Zhang and K. Deng, *ACS Catalysis*, 2015, **5**, 6529-6544.
15. Z. Zhang, B. Liu, K. Lv, J. Sun and K. Deng, *Green Chemistry*, 2014, **16**, 2762-2770.
16. N. Jacquel, R. Saint-Loup, J.-P. Pascault, A. Rousseau and F. Fenouillot, *Polymer*, 2015, **59**, 234-242.
17. S. Rajendran, R. Raghunathan, I. Hevus, R. Krishnan, A. Ugrinov, M. P. Sibi, D. C. Webster and J. Sivaguru, *Angewandte Chemie International Edition*, 2015, **54**, 1159-1163.
18. C. H. R. M. Wilsens, N. J. M. Wullems, E. Gubbels, Y. Yao, S. Rastogi and B. A. J. Noordover, *Polymer Chemistry*, 2015, **6**, 2707-2716.
19. A. J. J. E. Eerhart, A. P. C. Faaij and M. K. Patel, *Energy & Environmental Science*, 2012, **5**, 6407-6422.
20. B. Saha, D. Gupta, M. M. Abu-Omar, A. Modak and A. Bhaumik, *Journal of Catalysis*, 2013, **299**, 316-320.
21. M. E. Davis, *Top Catal*, 2015, **58**, 405-409.
22. A. Gandini, A. J. D. Silvestre, C. P. Neto, A. F. Sousa and M. Gomes, *Journal of Polymer Science Part A: Polymer Chemistry*, 2009, **47**, 295-298.
23. T. Miura, H. Kakinuma, T. Kawano and H. Matsuhisa, *Journal*, 2008.
24. W. P. Dijkman, D. E. Groothuis and M. W. Fraaije, *Angewandte Chemie International Edition*, 2014, **53**, 6515-6518.
25. F. Koopman, N. Wierckx, J. H. de Winde and H. J. Ruijssenaars, *Bioresource Technology*, 2010, **101**, 6291-6296.
26. S. M. McKenna, S. Leimkuhler, S. Herter, N. J. Turner and A. J. Carnell, *Green Chemistry*, 2015, **17**, 3271-3275.
27. Y. Y. Gorbanev, S. K. Klitgaard, J. M. Woodley, C. H. Christensen and A. Riisager, *ChemSusChem*, 2009, **2**, 672-675.
28. O. Casanova, S. Iborra and A. Corma, *ChemSusChem*, 2009, **2**, 1138-1144.
29. S. E. Davis, L. R. Houk, E. C. Tamargo, A. K. Datye and R. J. Davis, *Catalysis Today*, 2011, **160**, 55-60.
30. N. K. Gupta, S. Nishimura, A. Takagaki and K. Ebitani, *Green Chemistry*, 2011, **13**, 824-827.
31. X. Wan, C. Zhou, J. Chen, W. Deng, Q. Zhang, Y. Yang and Y. Wang, *ACS Catalysis*, 2014, **4**, 2175-2185.
32. G. Yi, S. P. Teong and Y. Zhang, *Green Chemistry*, 2016, **18**, 979-983.
33. M. Lilga, R. Hallen and M. Gray, *Top Catal*, 2010, **53**, 1264-1269.
34. J. Artz and R. Palkovits, *ChemSusChem*, 2015, **8**, 3832-3838.
35. H. Ait Rass, N. Essayem and M. Besson, *ChemSusChem*, 2015, **8**, 1206-1217.
36. L. Ardemani, G. Cibin, A. J. Dent, M. A. Isaacs, G. Kyriakou, A. F. Lee, C. M. A. Parlett, S. A. Parry and K. Wilson, *Chemical Science*, 2015, **6**, 4940-4945.
37. C. A. Antonyraj, J. Jeong, B. Kim, S. Shin, S. Kim, K.-Y. Lee and J. K. Cho, *Journal of Industrial and Engineering Chemistry*, 2013, **19**, 1056-1059.
38. M. E. Zakrzewska, E. Bogel-Łukasik and R. Bogel-Łukasik, *Chemical Reviews*, 2011, **111**, 397-417.
39. Y. Gorbanev, S. Kegnæs and A. Riisager, *Top Catal*, 2011, **54**, 1318-1324.
40. A. Takagaki, S. Nishimura and K. Ebitani, *Catal Surv Asia*, 2012, **16**, 164-182.
41. T. Ståhlberg, E. Eyjólfsdóttir, Y. Gorbanev, I. Sádaba and A. Riisager, *Catal Lett*, 2012, **142**, 1089-1097.
42. P. W. Menezes, A. Indra, N. R. Sahraie, A. Bergmann, P. Strasser and M. Driess, *ChemSusChem*, 2015, **8**, 164-171.
43. W. Partenheimer and Vladimir V. Grushin, *Advanced Synthesis & Catalysis*, 2001, **343**, 102-111.
44. K.-T. Li and S.-W. Li, *Applied Catalysis A: General*, 2008, **340**, 271-277.
45. T. Y. Ma, Y. Zheng, S. Dai, M. Jaroniec and S. Z. Qiao, *Journal of Materials Chemistry A*, 2014, **2**, 8676-8682.
46. M. Qiu, S. Zhan, H. Yu, D. Zhu and S. Wang, *Nanoscale*, 2015, **7**, 2568-2577.
47. X. Cao, J. Wu, C. Jin, J. Tian, P. Strasser and R. Yang, *ACS Catalysis*, 2015, **5**, 4890-4896.

View Article Online
DOI: 10.1039/C7GC00027H

Table of Contents:

COMMUNICATION

$MnCo_2O_4$ Spinels Supported Ruthenium Catalyst for Air-Oxidation of HMF to FDCA under Aqueous Phase and Base-Free Conditions